Investigating the Compatibility of IRI and ASAPS Models in Predicting the f$_o$F2 Ionospheric Parameter over the Mid Latitude Region

Ja'far M. Ja'far, Khalid A. Hadi

Department of Astronomy and Space, College of Science, University of Baghdad, Baghdad, Iraq

Abstract

In this research, an investigation for the compatibility of the IRI-2016 and ASAPS international models was conducted to evaluate their accuracy in predicting the ionospheric critical frequency parameter (f$_o$F2) for the years 2009 and 2014 that represent the minimum and maximum years of solar cycle 24. The calculations of the monthly average f$_o$F2 values were performed for three different selected stations distributed over the mid-latitude region. These stations are Athens - Greece (23.7^o E, 37.9 ^{o} N), El Arenosillo - Spain (-6.78 ^{o} E, 37.09 ^{o} N), and Je Ju - South Korea (124.53 ^{o} E, 33.6 ^{o} N). The calculated values using the two tested models were compared with the observed f$_o$F2 datasets for each of the three selected locations. The results showed that the two tested models gave good and close results for all selected stations compared to the observed data for the studied period of time. At the minimum solar cycle 24, the ASAPS model showed in general better values than the IRI-2016 model at Athens, El Arenosillo and Je Ju stations for all tested methods. At maximum solar cycle 24, the IRI-2016 model showed higher and closer values to the observed data at Athens and El Arenosillo stations, while the ASAPS model showed better values at Je Ju station.

Keywords: Ionospheric Parameters, Critical Frequency, IRI-2016 Model, ASAPS Model

التحقيق في توافق نماذج IRI–2016 و ASAPS في التنبؤ بمعلمة f$_o$F2 الأيونوسفيرية فوق منطقة خط العرض الوسطى

جعفر محمد جعفر*، خالد عبد الكريم هادي

قسم الفلك والفضاء ، كلية العلوم ، جامعة بغداد ، بغداد ، العراق

ألخلاصه

في هذا البحث ، تم إجراء دراسة للتحقيق من توافق النماذج العالمية IRI–2016 و ASAPS في دقة التنبؤ بمعامل التردد الحرج للغلاف الأيوني (f$_o$F2) خلال العامين 2009 و 2014 اللذين يمثلان الحد الأدنى والحد الأقصى لسنوات الدورة الشمسية 24. تم إجراء حسابات متوسط معامل التردد الحرج الشهري لثلاث محطات مختارة موزعة في منطقة خطوط العرض الوسطى، وهذه المحطات هي أثينا – اليونان (23.7^o شرقاً ، 37.9^o شمالاً) ، إلأرينوسيلو – إسبانيا (– 6.78^o شرقاً، 37.09 شمالاً) و جيجو – كوريا الجنوبية (124.53^o شرقاً ، 33.6^o شمالاً). تمت مقارنة قيم معامل التردد الحرج المحسوبة باستخدام النموذجين المختبرين مع مجموعة بيانات (f$_o$F2) المرصودة لكل موقع من المواقع الثلاثة المختارة. أظهرت

_____

*Email: jafar.king.1995544@gmail.com

نتائج الدراسة أن النموذجين المختبرين قد أعطيا نتائج جيدة ودقيقة لجميع المحطات المختارة مقارنة بالبيانات

المرصودة خلال فترة الدراسة. في الحد الأدنى للدورة الشمسية 24، أظهر نموذج ASAPS بشكل عام قيماً

أفضل في محطات أثينا و إلأرينوسيلو و جيجو من قيم نموذج IRI-2016 ولجميع الطرق المختبرة ، بينما

في الدورة الشمسية القصوى 24 ، أظهر نموذج IRI-2016 قيماً أعلى وأقرب إلى البيانات المرصودة من تلك

القيم التي تم الحصول عليها من نموذج ASAPS في محطتي أثينا وإلأرينوسيلو، قيما أظهر نموذج

ASAPS قيماً أفضل من نموذج IRI-2016 في محطة جيجو.

Introduction

The ionosphere is one of the layers of the Earth's upper atmosphere, extending from about 50 km to 1000 km and higher, which constitutes less than 1% of the mass of the atmosphere that exceeds 100 km. The ionosphere is an electrically neutral layer which is ionized when solar radiation strikes the components of chemical substances to the atmosphere by displacing their electrons from atoms and molecules [1]. This process occurs on the illuminating side of the Sun towards the Earth. The shorter wavelengths of solar radiation (ultraviolet photons (EUV) and shorter X-rays) have sufficient energy to produce this ionization. The presence of these charged particles makes the upper atmosphere an electrical conductor that supports electric currents and affects radio waves [2]. According to the density of the electron and ionization, the ionosphere is classified into two main regions, the "topside region", which extends over the surface of the earth upwards from about 500 km to 1000 km, and the "bottom side region", which extends from 50 to 500 km above the surface of the earth. The bottom side of the ionosphere is divided into three specific regions according to the height and distribution of ions, which are regions D, E, and F. Each region is split into layers, called D, E, Es, F1, and F2 layers. The D layer, which extends over the surface of the earth approximately about 50-90 km, is mainly responsible for the partial absorption of high frequency radio waves [3]. The E layer is extending about 90-150 km. These layers can only reflect radio waves that have frequencies below 5 MHz [4]. Also, there is an unexpected layer, known as E-Sporadic (Es), with a height of 80 to 120 km [5, 6]. One of the most ionized layers of the ionosphere is the F layer, and it usually ranges about 140-500 km. The light coming from the sun causes this layer to split into two distinct layers; F1, located at an altitude of 150-250 km, and F2, which is the highest layer of the ionosphere and is located at an altitude of 250-400 km [7].

In 2014, Hadi *et al*. studied the variation of the ionospheric critical frequency of the F2-layer (f_oF2) over Athens city for the monthly period of the years 2011, 2012, 2013. An analytical investigation was conducted and a relationship between the monthly average f_oF2 values and the hourly time factor was expressed as a suggested mathematical formula [8]. Jeon *et al*. (2016) used the mean and standard deviation to analyze the seasonal and annual changes of f_oF2 as well as the relationships of F2 layer height at two sites in South Korea. The median and spring for the study of the ionosphere were used to ensure a more accurate analysis [9]. Mohammed (2016) studied the accuracy of predicting the hourly f_oF2 values using IRI-2012 and VOACAP models for three Iraqi cities during high solar activity. The results indicated that the accuracy of them increases for all hours during Spring and Summer and decreases during Winter and Autumn, especially at hours near to sunrise. Both models were shown to have the same accuracy. f_oF2 values predicted by VOACAP model were reported to be higher than those predicted by IRI- 2012 model for all seasons [10].

Ionospheric Critical Frequency Parameter

The ionosphere is characterized by a set of different parameters. One of the most important parameters and the most frequently used is the critical frequency parameter, which is considered to describe the state of change of the ionosphere. If an ionospheric layer possesses a distinct maximum in ionization, a radio frequency capable of just penetrating to this height is called the critical frequency of the layer. The critical frequency is the maximum frequency

of each layer of the ionosphere at which radio waves can be sent vertically and refracted back to the Earth. The foF2 is an important parameter for describing the state of ionospheric variation and defined as the highest frequency signal that will reflect directly back to its transmission location depending on the time of day and day of the sunspot cycle. It is related to the maximum electron density of F2 layer (NmF2), according to the following equation [11] [12]:

$$(f_oF2)^2 = \frac{N_mF2e^2}{4\varepsilon_o m\pi} \qquad \cdots (1)$$

where:
f_oF2: critical frequency of the F2 layer.
N_mF2: max. electron density of the F2 layer.
e: electron charge.
ε_o: vacuum permittivity.
M: mass of electron.

International Ionospheric Models

In this research, the Advanced Stand Alone Prediction System (ASAPS6) model and the International Reference Ionosphere (IRI-2016) model were selected as international models to verify the compatibility of the accuracy of predicting the ionospheric critical frequency parameter which will be generated using the adopted models with the observed data for Athens, El Arenosillo and Je Ju stations. IRI model defines the monthly averages of critical F2-layer frequencies in the existing ionosphere altitude range of 50Km to 1500km [13]. ASAPS provides forecasting of sky-wave communication system performance in the high-frequency (HF) radio spectrum (1 to 30MHz) and basic surface wave performance in the medium frequency (300kHz-3MHz) and low-HF (3-5MHz) range. It is based on the ionosphere model developed by the Space Weather Services and ITU-R/CCIR models [14].

Test and Results

In this work, a comparative study between the ASAPS and IRI-2016 models was conducted by investigating the compatibility of predicting the ionospheric critical frequency parameter generated using the two tested models for three different stations distributed on the mid-latitude region during the maximum and minimum years of the 24th solar cycle. The f_oF2 of the F2 ionosphere layer was adopted to make a comparison between the two selected models. The values of the critical frequency parameters (f_oF2) were calculated for each of the three selected sites using the two tested models and compared with the observed f_oF2 data values for the monthly times variations of 2009 and 2014, which represent the minimum and the maximum for the years of the solar cycle 24. The monthly calculations of the critical frequency parameter for the selected locations were made according to the available observational data within the study period. The three tested locations that spread over the mid-latitude zone are Athens (Greece), El Arenosillo (Spain), and Je Ju (South Korea), for which the location and geographical coordinates are illustrated in Figure 1 and Table 1.

Figure 1-Distribution of the selected stations over the middle latitude region.

Table 1-Geographical coordinates of the selected stations distributed within the Mid-latitude region

| Time | 2009 | | | | | | | | | | | |
	Jan	Feb	Mar	Apr	May	Jun	Jul	Aug	Sep	Oct	Nov	Dec
1	12	16	17	18	23	25	21	23	20	21	15	12
2	13	10	15	23	23	27	22	18	21	19	21	13
3	14	14	9	20	23	21	18	22	19	15	15	11
4	12	12	10	18	21	22	24	22	18	21	17	14
5	14	16	14	22	12	15	23	23	23	12	17	11
6	10	17	12	23	13	16	22	22	21	8	15	10
7	10	13	17	20	20	22	21	22	24	13	19	14
8	9	16	19	19	20	19	22	19	25	21	14	13
9	6	9	17	22	18	20	23	19	20	19	15	12
10	7	13	14	22	21	18	20	21	22	17	15	17
11	4	15	19	20	20	22	18	19	24	15	13	9
12	2	19	15	17	19	27	23	22	21	19	13	11
13	8	11	15	20	16	25	22	23	22	22	13	15
14	13	19	20	22	20	20	21	25	18	21	19	17
15	10	13	19	23	18	17	24	26	16	20	14	20
16	5	13	18	17	20	23	23	26	18	21	13	14
17	12	12	21	13	15	23	20	24	22	18	8	11
18	8	20	22	18	23	22	19	25	25	17	18	17
19	9	16	22	20	20	20	19	24	24	22	17	14
20	12	10	21	18	24	17	20	25	20	19	19	12
21	9	18	22	17	19	17	20	19	20	15	17	12
22	13	12	15	20	20	17	19	23	23	16	11	11
23	12	10	18	21	23	23	20	23	16	20	14	17
24	10	12	19	18	22	22	23	21	25	13	9	14
25	8	10	16	17	21	23	23	21	24	17	17	12
26	17	14	12	17	20	20	24	23	23	16	22	17
27	14	9	17	21	22	18	23	26	21	21	15	14
28	11	16	14	16	17	20	24	22	20	22	15	19
29	8		18	20	21	21	23	21	15	18	9	14
30	14		17	24	19	21	25	21	18	24	13	7
31	11		19		17		22	21		22		11

The implementation of the IRI-2016 and ASAPS models needs several input parameters, including the monthly sunspot number (SSN) of the tested years. In this work, daily sunspot numbers were used to calculate the daily variation of the critical frequency parameter using the tested models. Table (2) presents a daily sunspot numbers for the tow adopted years (2009 & 2014).

Table 2- The daily sunspot numbers (SSN) for the years 2009 & 2014 [15].

| Time | 2014 | | | | | | | | | | | |
	Jan	Feb	Mar	Apr	May	Jun	Jul	Aug	Sep	Oct	Nov	Dec
1	13	9	7	21	16	15	18	21	15	14	15	3
2	11	15	12	20	19	15	17	17	16	14	15	5
3	10	17	12	16	17	14	14	16	15	16	15	6
4	8	16	12	9	17	11	14	18	14	13	14	6
5	14	18	13	14	18	14	11	18	13	8	16	9
6	15	13	19	16	17	15	12	17	13	13	13	13
7	15	11	15	19	14	13	16	19	14	14	13	9
8	16	6	15	21	9	16	12	12	18	11	18	16
9	12	14	17	20	19	18	8	15	14	17	13	14
10	19	13	20	18	12	19	12	13	14	20	17	15
11	13	12	17	21	15	17	9	22	11	18	17	9
12	20	15	21	17	16	18	13	15	12	16	12	6
13	16	12	17	12	18	20	9	18	14	13	15	6
14	9	11	21	16	16	15	20	12	11	16	12	13
15	9	12	14	19	15	15	16	17	11	13	13	11
16	9	14	14	15	17	16	20	15	17	15	10	13
17	16	18	14	18	15	13	22	12	14	16	13	9
18	16	13	12	12	16	14	19	18	13	17	8	8
19	13	14	19	14	20	17	12	14	16	17	9	11
20	7	12	19	10	20	16	15	18	9	17	13	13
21	7	17	20	12	16	14	15	17	12	13	14	13
22	15	13	12	18	20	11	18	17	15	11	15	9
23	14	16	15	17	17	20	20	14	15	6	14	11
24	15	18	18	17	18	19	18	15	13	11	19	10
25	8	17	17	17	14	18	19	12	15	9	11	16
26	12	16	12	18	13	18	13	7	9	12	4	11
27	17	12	16	15	9	15	16	17	16	17	10	9
28	11	10	18	13	11	13	17	16	14	17	15	16
29	12		17	14	14	14	16	17	16	11	17	16
30	9		17	17	18	16	16	11	20	19	7	15
31	17		21		17		20	16		16		10

The calculations of the critical frequency parameter using IRI-2016 model were made directly from the model, whereas in the ASAPS model they were made by extracting the data values of the maximum usable frequency parameter (MUF) then converting them to f_oF2 using the following equation [16]:

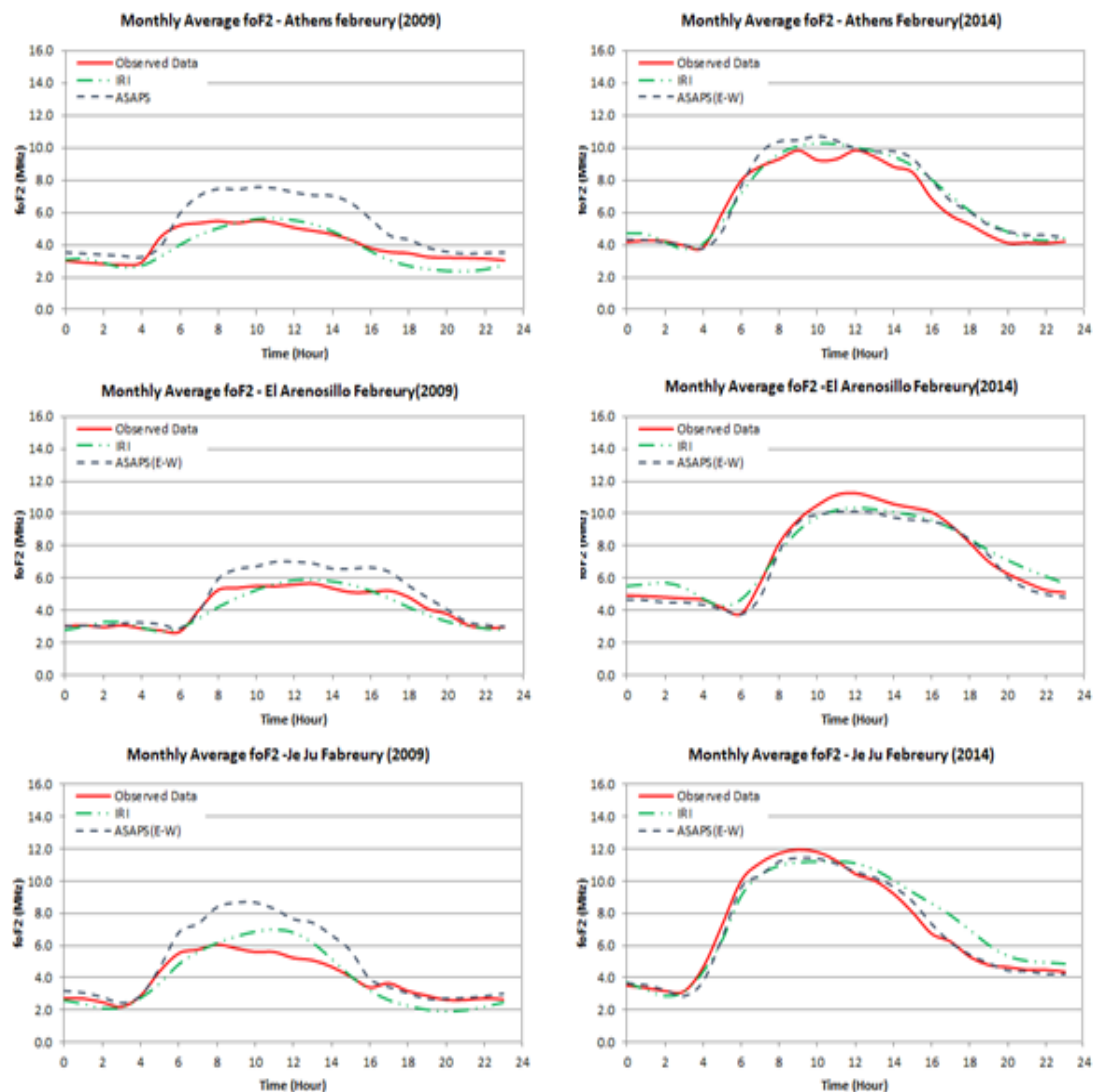$$f_oF2 = MUF * \sqrt{1 - (\frac{R}{R+h})^2} \qquad \qquad \dots (2)$$

where:

MUF: maximum usable frequency.

f_o: critical frequency.

R: radius of the Earth (R $_\oplus$ = 6372 Km).

h: height of the ionosphere (typical height of the F2 ionospheric layer is about 400 Km).

Figure 2-Samples of the monthly variations of the f_oF2 parameter for Athens, El Arenosillo, and Je Ju stations during the years (2009 and 2014) using IRI-2016 and ASAPS models, compared with the observed data.

The monthly predicted f_oF2 values (theoretical) for the F2 ionospheric layer (height 400 Km) for the three selected stations, Athens (23.7° E, 37.9° N), El Arenosillo (-6.78° E, 37.09° N) and Je Ju (124.53° E, 33.6° N), were calculated using the two tested models for the two selected years (2009 and 2014) that represented the maximum and minimum years of solar cycle 24. Figure 2 presents samples of the results of the monthly variations of the f_oF2 ionospheric parameter which were calculated using IRI-2016 and ASAPS models and their comparison with the observed data for the same period of time.

From the results that illustrated in Figure 2 for the three stations, it can be noticed that the values of f_oF2 vary with time, as the maximum value occurs during noon, then the values decrease and reach their minimum at sunrise and sunset. Time differences cause differences in frequency values as a result of the interaction of solar radiation with the components of the ionosphere layers.

Statistical Calculations

The statistical analysis for the observed and predicted f_oF2 datasets generated using IRI-2016 and ASAPS models was performed. The statistical calculations were conducted using the correlation coefficient (R), Root Mean Square Error (RMSE), Standard Deviation (STD), Mean Average (Mean (Ave.)), Mean Deviation (MD), Variance, Mean Difference (Mean Diff.), Mean Signed Deviation (MSD), Standard Error and Mean Absolute Deviation (MAD) statistical analysis methods. Samples of the statistical calculation results are presented in Tables (3), (4), (5), (6), (7), and (8).

Table 3-Statistical calculation results for the observed and predicted (theoretical) foF2 datasets of Athens station for the year 2009.

Month	R	RMSE	STD	Ave. Mean	MD	Variance	Mean Diff.	MSD	Stand. Error	MAD
Observed-IRI										
January	0.950	0.355	1.121	3.604	0.997	0.126	0.085	0.126	0.716	0.997
February	0.912	0.551	1.190	3.770	1.062	0.304	0.269	0.304	0.716	1.062
March	0.922	0.550	1.385	4.183	1.258	0.303	-0.017	0.303	0.716	1.258
April	0.872	0.694	1.410	4.594	1.272	0.481	-0.061	0.481	0.716	1.272
May	0.868	0.562	1.135	4.941	0.987	0.315	-0.086	0.315	0.716	0.987
June	0.768	0.674	0.925	5.004	0.773	0.454	0.134	0.454	0.716	0.773
July	0.901	0.388	0.890	4.763	0.752	0.151	-0.076	0.151	0.716	0.752
August	0.925	0.459	0.997	4.702	0.867	0.211	-0.264	0.211	0.716	0.867
September	0.933	0.530	1.233	4.739	1.119	0.281	-0.301	0.281	0.716	1.119
October	0.963	0.522	1.654	4.724	1.502	0.272	-0.192	0.272	0.716	1.502
November	0.953	0.565	1.576	4.256	1.423	0.319	-0.238	0.319	0.716	1.423
December	0.945	0.467	1.325	3.927	1.182	0.218	-0.150	0.218	0.716	1.182
Observed-ASAPS										
January	0.963	1.094	1.526	4.615	1.237	1.198	-0.926	1.198	0.747	1.378
February	0.937	1.393	1.733	5.158	1.629	1.942	-1.119	1.942	0.747	1.615
March	0.970	1.505	1.937	5.386	1.951	2.265	-1.221	2.265	0.747	1.814
April	0.919	1.556	1.821	5.794	1.871	2.420	-1.261	2.420	0.747	1.638
May	0.867	1.593	1.306	6.312	1.602	2.537	-1.458	2.537	0.747	1.128
June	0.795	1.117	1.147	6.016	1.332	1.248	-0.877	1.248	0.747	0.955
July	0.940	1.121	1.285	5.657	1.392	1.256	-0.970	1.256	0.747	1.110
August	0.944	1.420	1.537	5.636	1.611	2.015	-1.198	2.015	0.747	1.321
September	0.956	1.280	1.768	5.469	1.749	1.638	-1.031	1.638	0.747	1.614
October	0.958	1.650	2.739	5.337	2.595	2.721	-0.805	2.721	0.747	2.564
November	0.965	1.389	2.090	5.084	1.869	1.929	-1.066	1.929	0.747	1.955
December	0.957	1.197	1.645	4.785	1.394	1.433	-1.008	1.433	0.747	1.525

Table 4-Statistical calculation results for the observed and theoretical (predicted) f_oF2 datasets of Athens station for the year 2014.

Month	R	RMSE	STD	Ave. Mean	MD	Variance	Mean Diff.	MSD	Stand. Error	MAD
				Observed-IRI						
January	0.973	0.947	2.433	6.212	2.204	0.897	-0.763	0.897	0.716	2.204
February	0.978	0.626	2.436	6.920	2.209	0.392	-0.386	0.392	0.716	2.209
March	0.989	0.458	2.291	7.693	2.075	0.210	0.305	0.210	0.716	2.075
April	0.990	0.276	1.917	8.216	1.720	0.076	-0.043	0.076	0.716	1.720
May	0.980	0.491	1.308	8.188	1.143	0.241	-0.417	0.241	0.716	1.143
June	0.949	0.540	0.869	7.799	0.719	0.292	-0.457	0.292	0.716	0.719
July	0.952	0.703	0.921	7.559	0.763	0.494	-0.646	0.494	0.716	0.763
August	0.974	0.902	1.263	7.535	1.104	0.814	-0.854	0.814	0.716	1.104
September	0.979	0.682	1.667	7.584	1.506	0.465	-0.592	0.465	0.716	1.506
December	0.979	0.706	2.499	6.230	2.257	0.499	-0.088	0.499	0.716	2.257
				Observed-ASAPS						
January	0.972	1.079	2.418	6.367	2.173	1.165	-0.918	1.165	0.747	2.186
February	0.979	0.747	2.642	7.032	2.418	0.559	-0.498	0.559	0.747	2.427
March	0.984	0.566	2.467	7.632	2.298	0.320	0.366	0.320	0.747	2.298
April	0.980	0.578	1.965	7.739	1.744	0.334	0.434	0.334	0.747	1.784
May	0.988	0.233	1.364	7.833	1.202	0.054	-0.062	0.054	0.747	1.185
June	0.869	0.491	0.987	7.428	0.748	0.241	-0.086	0.241	0.747	0.826
July	0.957	0.371	1.123	6.880	0.947	0.138	0.034	0.138	0.747	0.971
August	0.983	0.438	1.412	6.959	1.143	0.192	-0.279	0.192	0.747	1.234
September	0.984	0.447	1.908	7.041	1.700	0.199	-0.049	0.199	0.747	1.745
December	0.982	0.759	2.363	6.188	2.165	0.576	-0.046	0.576	0.747	2.162

Table 5- Statistical calculation results for the observed and theoretical (predicted) foF2 datasets of El Arenosillo station for the year 2009.

Month	R	RMSE	STD	Ave. Mean	MD	Variance	Mean Diff.	MSD	Stand. Error	MAD
				Observed-IRI						
January	0.969	1.104	2.213	6.686	1.974	1.220	-0.951	1.220	0.716	1.974
February	0.989	0.643	2.084	7.447	1.854	0.414	-0.068	0.414	0.716	1.854
March	0.989	1.167	1.945	8.209	1.723	1.362	1.028	1.362	0.716	1.723
April	0.961	0.655	1.680	8.522	1.484	0.429	0.163	0.429	0.716	1.484
May	0.924	0.490	1.154	8.371	0.972	0.240	-0.042	0.240	0.716	0.972
June	0.948	0.356	0.791	7.885	0.657	0.126	0.042	0.126	0.716	0.657
July	0.951	0.270	0.828	7.668	0.687	0.073	-0.067	0.073	0.716	0.687
August	0.967	0.630	1.175	7.758	1.022	0.397	-0.517	0.397	0.716	1.022
September	0.986	0.529	1.521	7.832	1.361	0.280	-0.232	0.280	0.716	1.361
October	0.979	0.954	2.005	8.024	1.811	0.911	-0.198	0.911	0.716	1.811
November	0.979	1.037	2.155	7.666	1.936	1.075	-0.485	1.075	0.716	1.936
December	0.977	0.914	2.203	6.913	1.970	0.835	-0.221	0.835	0.716	1.970
				Observed-ASAPS						
January	0.978	0.921	2.591	6.456	2.367	0.849	-0.722	0.849	0.747	2.342
February	0.992	0.520	2.463	7.005	2.292	0.270	0.374	0.270	0.747	2.290
March	0.971	2.018	2.358	7.298	2.203	4.072	1.938	4.072	0.747	2.203
April	0.971	1.392	1.845	7.389	1.738	1.937	1.296	1.937	0.747	1.675
May	0.927	1.094	1.275	7.346	1.267	1.197	0.983	1.197	0.747	1.083
June	0.935	0.833	1.002	7.173	0.945	0.693	0.753	0.693	0.747	0.823
July	0.969	0.772	1.038	6.885	0.987	0.595	0.717	0.595	0.747	0.856
August	0.927	0.615	1.334	6.883	1.148	0.378	0.357	0.378	0.747	1.168
September	0.978	0.770	1.959	6.943	1.724	0.593	0.658	0.593	0.747	1.798
October	0.985	0.577	2.746	7.507	2.597	0.333	0.319	0.333	0.747	2.575
November	0.985	0.552	2.724	6.986	2.617	0.305	0.195	0.305	0.747	2.547
December	0.989	0.667	2.502	6.355	2.378	0.445	0.337	0.445	0.747	2.301

Table 6-Statistical calculation results for the observed and theoretical (predicted) foF2 datasets of El Arenosillo station for the year 2014.

| Month	R	RMSE	STD	Ave. Mean	MD	Variance	Mean Diff.	MSD	Stand. Error	MAD
Observed-IRI										
January										
February	0.947	0.739	1.884	3.889	1.685	0.546	0.033	0.546	0.716	1.685
March	0.967	0.741	2.102	4.481	1.890	0.549	-0.135	0.549	0.716	1.890
April	0.899	1.059	2.035	4.970	1.810	1.122	-0.461	1.122	0.716	1.810
May	0.894	0.905	1.420	5.188	1.161	0.819	-0.656	0.819	0.716	1.161
June	0.846	0.710	0.960	5.255	0.764	0.505	-0.400	0.505	0.716	0.764
July	0.928	0.452	0.864	4.927	0.705	0.205	-0.172	0.205	0.716	0.705
August	0.907	0.581	1.052	4.828	0.881	0.338	-0.381	0.338	0.716	0.881
September	0.893	0.811	1.550	5.020	1.393	0.658	-0.415	0.658	0.716	1.393
October	0.937	1.063	2.042	5.121	1.845	1.129	-0.549	1.129	0.716	1.845
November	0.970	0.748	2.120	4.673	1.905	0.559	-0.267	0.559	0.716	1.905
December	0.958	0.647	1.775	3.967	1.602	0.418	0.004	0.418	0.716	1.602
Observed-ASAPS										
January										
February	0.973	1.507	2.370	4.959	2.057	2.270	-1.038	2.270	0.747	2.169
March	0.975	1.843	2.744	5.670	2.451	3.398	-1.324	3.398	0.747	2.497
April	0.940	2.313	2.636	6.391	2.529	5.352	-1.882	5.352	0.747	2.373
May	0.934	2.046	1.861	6.422	1.829	4.187	-1.890	4.187	0.747	1.536
June	0.913	1.414	1.166	6.190	1.237	2.000	-1.334	2.000	0.747	0.975
July	0.947	1.064	1.089	5.761	1.184	1.132	-1.006	1.132	0.747	0.991
August	0.965	1.371	1.456	5.712	1.516	1.879	-1.264	1.879	0.747	1.313
September	0.962	1.459	1.748	5.919	1.744	2.128	-1.313	2.128	0.747	1.595
October	0.969	2.039	2.689	6.038	2.441	4.157	-1.466	4.157	0.747	2.484
November	0.980	1.525	2.578	5.495	2.306	2.324	-1.089	2.324	0.747	2.375
December	0.975	1.174	2.180	4.657	1.904	1.378	-0.685	1.378	0.747	2.019

Table 7-Statistical calculation results for the observed and theoretical (predicted) f_oF2 datasets of Je Ju station for the year 2009.

Month	R	RMSE	STD	Ave. Mean	MD	Variance	Mean Diff.	MSD	Stand. Error	MAD
Observed-IRI										
January	0.959	1.039	2.834	6.692	2.517	1.080	-0.675	1.080	0.716	2.517
February	0.963	0.884	3.006	7.438	2.693	0.781	-0.246	0.781	0.716	2.693
March	0.991	0.510	2.881	8.357	2.533	0.260	0.304	0.260	0.716	2.533
April	0.962	0.662	2.420	9.083	2.025	0.439	0.060	0.439	0.716	2.025
May	0.917	0.716	1.540	8.943	1.218	0.513	-0.387	0.513	0.716	1.218
June	0.977	0.518	1.906	9.438	1.678	0.269	-0.163	0.269	0.716	1.678
July	0.736	0.838	0.985	7.987	0.769	0.702	-0.497	0.702	0.716	0.769
August	0.959	1.055	1.207	8.071	1.023	1.114	-0.999	1.114	0.716	1.023
September	0.974	1.070	1.854	8.414	1.671	1.144	-0.987	1.144	0.716	1.671
October	0.953	1.039	2.554	8.539	2.302	1.079	-0.609	1.079	0.716	2.302
November	0.969	0.917	2.725	7.699	2.457	0.840	-0.499	0.840	0.716	2.457
December	0.970	0.843	2.752	6.830	2.477	0.710	-0.017	0.710	0.716	2.477
Observed-ASAPS										
January	0.980	0.803	2.900	6.556	2.634	0.645	-0.539	0.645	0.747	2.622
February	0.992	0.422	3.137	7.071	2.884	0.178	0.121	0.178	0.747	2.847
March	0.976	1.015	3.241	7.932	2.991	1.030	0.729	1.030	0.747	2.956
April	0.976	0.900	2.657	8.459	2.363	0.809	0.684	0.809	0.747	2.409
May	0.946	0.678	1.700	8.196	1.496	0.460	0.360	0.460	0.747	1.403
June	0.968	0.756	2.265	8.761	2.068	0.572	0.514	0.572	0.747	2.061
July	0.859	0.641	1.124	7.193	1.053	0.411	0.297	0.411	0.747	0.958
August	0.966	0.535	1.396	7.386	1.216	0.286	-0.314	0.286	0.747	1.235
September	0.975	0.574	2.038	7.752	1.858	0.330	-0.326	0.330	0.747	1.877
October	0.982	0.631	3.074	8.135	2.852	0.399	-0.204	0.399	0.747	2.825
November	0.991	0.489	3.097	7.479	2.846	0.239	-0.279	0.239	0.747	2.827
December	0.989	0.682	2.879	6.403	2.701	0.465	0.410	0.465	0.747	2.656

Table 8-Statistical calculation results for the observed and theoretical (predicted) foF2 datasets of Je Ju station for the year 2014.

Month	R	RMSE	STD	Ave. Mean	MD	Variance	Mean Diff.	MSD	Stand. Error	MAD
Observed-IRI										
January	0.959	1.039	2.834	6.692	2.517	1.080	-0.675	1.080	0.716	2.517
February	0.963	0.884	3.006	7.438	2.693	0.781	-0.246	0.781	0.716	2.693
March	0.991	0.510	2.881	8.357	2.533	0.260	0.304	0.260	0.716	2.533
April	0.962	0.662	2.420	9.083	2.025	0.439	0.060	0.439	0.716	2.025
May	0.917	0.716	1.540	8.943	1.218	0.513	-0.387	0.513	0.716	1.218
June	0.977	0.518	1.906	9.438	1.678	0.269	-0.163	0.269	0.716	1.678
July	0.736	0.838	0.985	7.987	0.769	0.702	-0.497	0.702	0.716	0.769
August	0.959	1.055	1.207	8.071	1.023	1.114	-0.999	1.114	0.716	1.023
September	0.974	1.070	1.854	8.414	1.671	1.144	-0.987	1.144	0.716	1.671
October	0.953	1.039	2.554	8.539	2.302	1.079	-0.609	1.079	0.716	2.302
November	0.969	0.917	2.725	7.699	2.457	0.840	-0.499	0.840	0.716	2.457
December	0.970	0.843	2.752	6.830	2.477	0.710	-0.017	0.710	0.716	2.477
Observed-ASAPS										
January	0.980	0.803	2.900	6.556	2.634	0.645	-0.539	0.645	0.747	2.622
February	0.992	0.422	3.137	7.071	2.884	0.178	0.121	0.178	0.747	2.847
March	0.976	1.015	3.241	7.932	2.991	1.030	0.729	1.030	0.747	2.956
April	0.976	0.900	2.657	8.459	2.363	0.809	0.684	0.809	0.747	2.409
May	0.946	0.678	1.700	8.196	1.496	0.460	0.360	0.460	0.747	1.403
June	0.968	0.756	2.265	8.761	2.068	0.572	0.514	0.572	0.747	2.061
July	0.859	0.641	1.124	7.193	1.053	0.411	0.297	0.411	0.747	0.958
August	0.966	0.535	1.396	7.386	1.216	0.286	-0.314	0.286	0.747	1.235
September	0.975	0.574	2.038	7.752	1.858	0.330	-0.326	0.330	0.747	1.877
October	0.982	0.631	3.074	8.135	2.852	0.399	-0.204	0.399	0.747	2.825
November	0.991	0.489	3.097	7.479	2.846	0.239	-0.279	0.239	0.747	2.827
December	0.989	0.682	2.879	6.403	2.701	0.465	0.410	0.465	0.747	2.656

Samples of the monthly statistical correlation results between the observed and predicted f_oF2 ionospheric parameter values that were generated using IRI-2016 and ASAPS models are shown in Figure 3. Also, samples of the statistical analysis resulted for the statistical methods of Difference Residual and Absolute Residual between observed and predicted f_oF2 dataare presented in Figure 4.
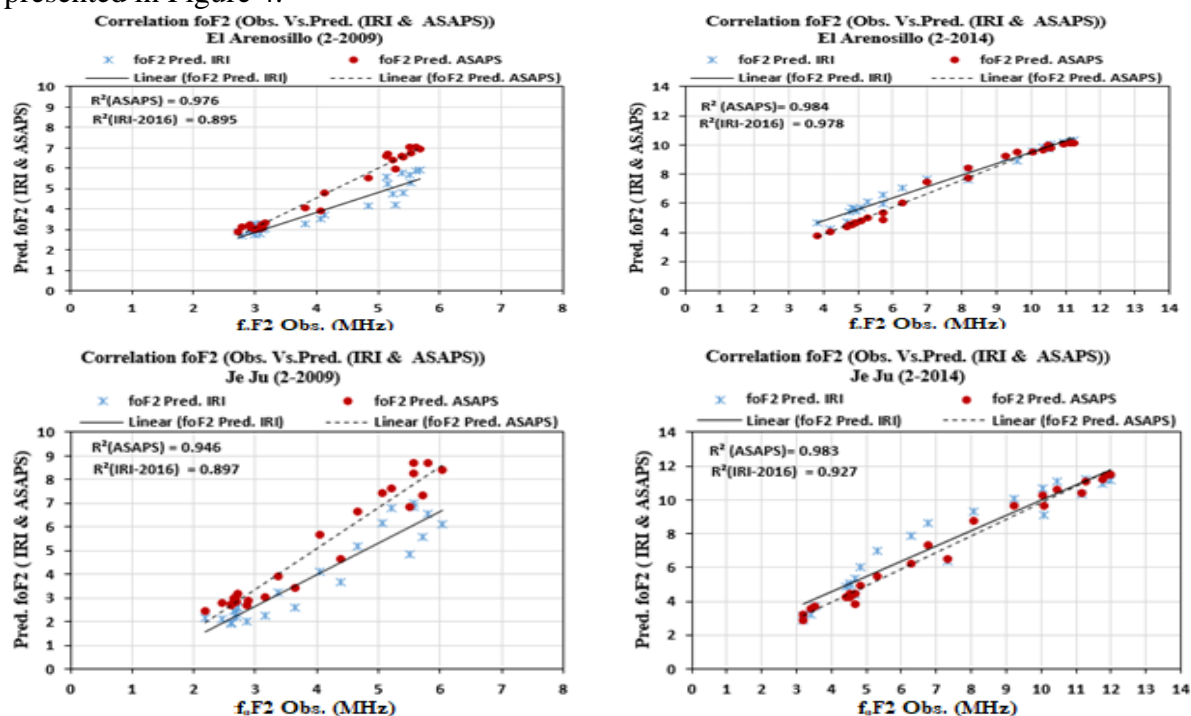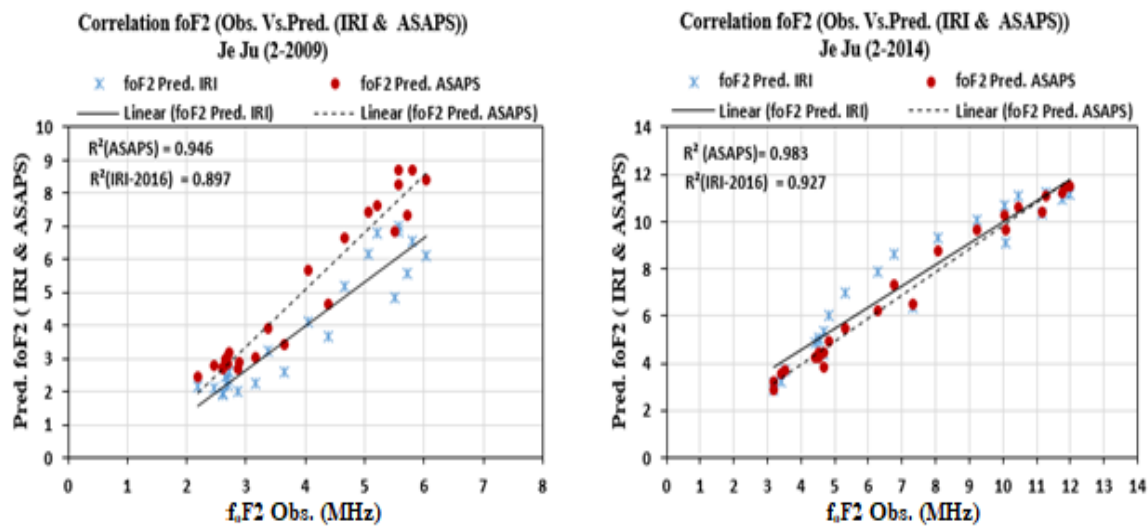
Figures 3-Samples of the monthly statistical correlation between observed and predicted foF2 data using IRI and ASAPS models for Athens, El Arenosillo and Je Ju stations for years 2009 and 2014.
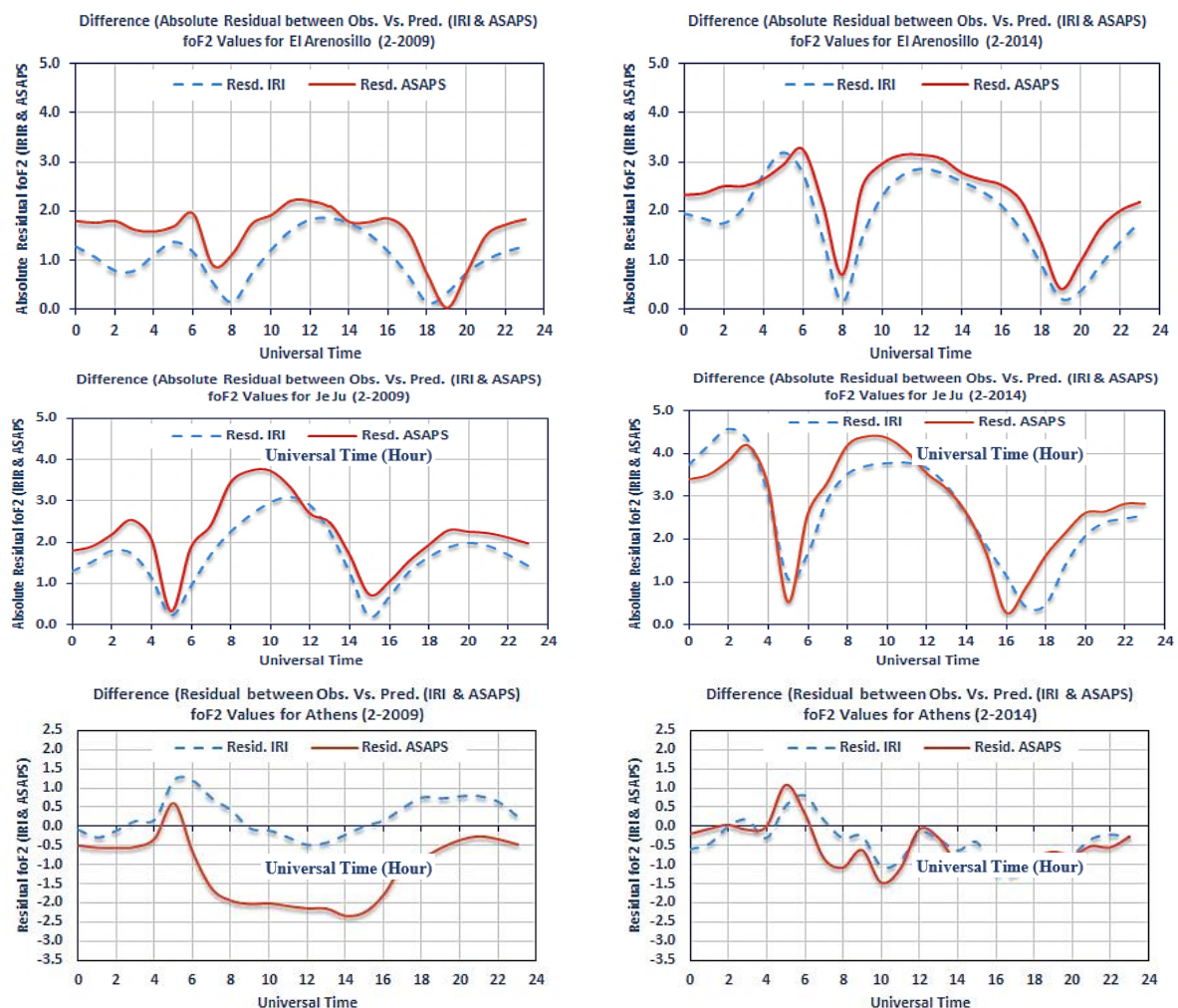
Figure 4-Samples of the Residual and Absolute residual methods between observed and predicted foF2 data for Athens, El Arenosillo and Je Ju stations for years 2009 and 2014.

The statistical calculation results for the observed and predicted (theoretical) f_oF2 datasets of the three stations is presented in Tables (3) - (8). While the behavior of the calculated statistical analysis results for IRI and ASAPS models for the three stations for the years 2009 and 2014 have been shown in Figures (3) and (4).

The calculations of the monthly statistical correlation coefficients revealed that the predicted ionosphere parameter values using ASAPS model reflect somewhat better results compared to the observed data from the results obtained from the IRI-2016 model for all the stations, except for Athens station which showed better results for the IRI-2016 model in 2014. While the results of the average monthly correlations showed that the ASAPS model gave better results than those achieved from IRI-2016 model during 2009 (during the minimum solar cycle) and for all tested stations. The calculations of year 2014 (the maximum solar cycle) showed that the model IRI-2016 gave better results for Athens and EI Arenosillo stations, in contrast to Je Ju station, where the results of the ASAPS model were better than those calculated according to the IRI-2016 model.

Corr. Coeff. (R)	2009				2014			
	IRI-2016		ASAPS		IRI-2016		ASAPS	
Athens	Oct.	0.963	**Mar.**	**0.970**	**Apr.**	**0.990**	May	0.988
El Arenosillo	Oct.	0.979	**Feb.**	**0.988**	Feb.	0.989	**Feb.**	**0.992**
Je Ju	Nov.	0.970	**Nov.**	**0.980**	Mar.	0.991	**Feb.**	**0.992**
Average Monthly Correlation								
Tested Locations	2009				2014			
	IRI-2016		ASAPS		IRI-2016		ASAPS	
Athens	0.909		**0.931**		**0.974**		0.968	
El Arenosillo	0.923		**0.965**		**0.968**		0.9 67	
Je Ju	0.922		**0.957**		0.944		**0.967**	

The results of the monthly statistical calculations of f_oF2 and the statistical analysis results for the RMSE, MAD, MSD, Res. and Abs. Res. statistical methods between observed and predicted f_oF2 values also showed that IRI-2016 model is more efficient in predicting f_oF2 parameter for the three tested stations for the year 2009, providing better and closer results to the observed data than those obtained by ASAPS model. While the statistical analysis results for the statistical parameters RMSE, Mean Avg, Variance, MSD for the three stations for year 2014 showed that the best results were obtained by ASAPS model for Athens and Je Ju stations. The statistical calculations using the parameters of RMSE, STD, MD, Variance, Mean Diff, MSD and MAD for El Arenosillo station showed that the best results were generated by IRI-2016 model, as illustrated in the following Tables.

Statistical Parameter	2009					
	Athens		El Arenosillo		Je Ju	
	IRI-2016	ASAPS	IRI-2016	ASAPS	IRI-2016	ASAPS
RMSE	0.526	1.359	0.589	0.984	0.769	1.614
STD	1.237	1.711	1.255	1.810	1.619	2.047
Mean Avg.	4.434	5.437	4.624	5.310	4.756	5.747
MD	1.099	1.686	1.110	1.716	1.422	1.927
Variance	0.286	1.883	0.362	1.005	0.623	2.746

Mean Diff.	-0.075	-1.078		-0.035	-0.721	-0.309	-1.299
MSD	0.286	1.883		0.362	1.005	0.623	2.746
Stand Error	0.716	0.747		0.716	0.747	0.716	0.747
MAD	1.099	1.551		1.110	1.626	1.422	1.848
Statistical Parameter	**2014**						
	Athens			**El Arenosillo**		**Je Ju**	
	IRI-2016	**ASAPS**		**IRI-2016**	**ASAPS**	**IRI-2016**	**ASAPS**
RMSE	0.633	0.571		0.729	0.894	0.841	0.677
STD	1.761	1.865		1.646	1.986	2.222	2.459
Mean Avg.	7.394	7.110		7.748	7.019	8.124	7.610
MD	1.570	1.654		1.454	1.855	1.947	2.247
Variance	0.438	0.378		0.613	0.972	0.744	0.485
Mean Diff.	-0.394	-0.110		-0.129	0.600	-0.393	0.121
MSD	0.438	0.378		0.613	0.972	0.744	0.485
Stand Error	0.716	0.747		0.716	0.747	0.716	0.747
MAD	1.570	1.682		1.454	1.805	1.947	2.223

Conclusions

The results of the conducted study showed that the two tested models gave good and close results for all selected stations compared to the observed data for the studied period of time. The calculations of the statistical correlation coefficients for the monthly predicted f_oF2 parameter datasets for the year 2009 showed that the predicted f_oF2 results using ASAPS model for all stations were better than the results obtained from IRI-2016 model, while those for the year 2014 showed that ASAPS model was somewhat results compared to IRI-2016 model for EI Arenosillo and Je Ju stations. The results of the average monthly correlations showed that the ASAPS model gave better results than those achieved by IRI-2016 model during 2009 (during the minimum solar cycle) for all the stations. The calculations of the average monthly correlations for year 2014 (the maximum solar cycle) showed that the ASAPS model gave better results than those calculated according to IRI-2016 model for Je Ju station, while the IRI-2016 model showed better results for Athens and EI Arenosillo stations. The best results of the monthly f_oF2 parameter values for all stations of the year (2009) were those predicted using the IRI-2016 model, which gave better and closer results to the observed data than those obtained from ASAPS model. The monthly f_oF2 parameter values for all stations of the year (2014) showed best results predicted using the IRI-2016 model, which gave better and closer results to the observed data than those obtained from ASAPS model. At the minimum solar cycle 24, in general, ASAPS model showed better values at Athens, El Arenosillo, and Je Ju stations than the ASAPS model for all tested methods. At maximum solar cycle 24, in general, IRI-2016 model showed higher and closer values to the observed data than those values obtained from ASAPS model at Athens and El Arenosillo stations, while the ASAPS model showed better values than IRI-2016 model at Je Ju station.

References
[1] Z. Aziz and K. A. Hadi, "Determination of Ionospheric Parameters Over Iraqi Zone", *Iraqi Journal of Science*. vol 54, no.2 , pp: 475-484, 2013.
[2] "Introduction to HF Radio Propagation" Australian Government – IPS Radio and Space Services, 2008.
[3] A. D. Khudhur and K. A. Hadi," Analytical Study for the Annual TEC Parameter Variations for the Solar Cycle 24 over Iraqi Zone", *Iraqi Journal of Science*, vol. 56, no. 3C, pp: 2694-2703,2015.

[4] Malik R A, Abdullah M, Abdullah S, Homam M J. "Comparison of maximum usable frequency (MUF) variability over Peninsular Malaysia with IRI model during the rise of solar cycle 24*", J Atmos Sol-Terr Phy*, vol. 138-139: pp. 87–92, 2016.

[5] J. Niu, L. B. Weng, X. Meng, H. X. Fang, "Morphology of Ionospheric Sporadic E Layer Intensity Based on COSMIC Occultation Data in the Midlatitude and Low-Latitude Regions", *Journal of Geophysical Research: Space Physics,* vol. 124, no. 6, 2019.

[6] K. A. Hadi, M. D. Abdulkareem, "The Suggested Reciprocal Relationship between Maximum, Minimum and Optimum Usable Frequency Parameters Over Iraqi Zone", *Baghdad Science Journal*, vol.17, no. 3, Supplement (September), pp. :1058-1070, 2020, DOI: http://dx.doi.org/10.21123/bsj. 2020.17.3(Suppl.).1058

[7] N. M. Maslin, *HF communications: A system approach, Pitman Publishing, London, Britain*, ISBN 0-273-02675-5, pp. 43, 2015.

[8] K. A. Hadi, A. Z. Azeez, A. D. Khdhur and R. A. Nasser, "Ionospheric Empirical Mathematical Formula to Forecast the Critical Frequency of F2-layer over Athens", *Global Research Analysis*, vol. 3, no. 4, ISSN No 2277 – 8160, April 2014.

[9] M. H. Jeon and C. H. Oh, "Analysis of Ionospheric foF2 by Solar Activity over the Korean Peninsula", *International Journal of Electrical and Computer Engineering*, vol. 6, no. 1, pp. 71-81, February 2016.

[10] F. A. Mohammed, " The Accuracy of Prediction for the Models IRI- 2012 and VOACAP in Measurements foF2 Over Iraq during High Solar Activity Level", *Iraqi Journal of Science*, vol. 57, no.3B, pp. 2131-2140, 2016.

[11] A. A. Hamied and K. A. Hadi, "Annual Behavior of Electron Density and Critical Frequency Parameters During Maximum and Minimum Years of Solar Cycles 22, 23 and 24", *J. Phys.: Conf. Ser*. 1818 012065, doi:10.1088/1742-6596/1818/1/012065, 2021.

[12] Z. Moˇsna, P. Sauli and O. Santol´ık, "Analysis of Critical Frequencies in the Ionosphere", *WDS'08 Proceedings of Contributed Papers, Part II, ISBN* 978-80-7378-066-1, pp. 172–177, 2008.

[13] D. Bilitza, International Reference Ionosphere, NASA/GSFC, Heliospheric Physics Lab., Code 672, Greenbelt, Maryland 20771 and Space Weather Lab., George MasonUniversity, Fairfax, Virginia, 2016.

[14] Space Weather Services, Australian Government Bureau of Metrology. [Online]. Available: https://www.sws.bom.gov.au/Products_and_Services/1/2

[15] The Sunspot Cycle, Marshall Space Flight Center, NASA, USA, November 2018.

[16] http://solarscience.msfc.nasa.gov/Sun

[17] R. A. Malik, M. Abdullah, S. Abdullah, M. J. Homam, "The influence of sunspot number on high frequency radio propagation." *IEEE Asia-Pacific Conference on Applied Electromagnetics* (APACE), pp. 107-110. IEEE, 2014.